



# Pion electro-production in the Roper region: planned experiment at the MAMI/A1 setup

S. Širca

Faculty of Mathematics and Physics, University of Ljubljana, 1000 Ljubljana, Slovenia  
Jožef Stefan Institute, 1000 Ljubljana, Slovenia

**Abstract.** This paper describes technical details of the experiment proposal submitted to the MAMI/ELSA Program Advisory Committee 2009 to study the structure of the Roper resonance by a measurement of recoil proton polarization components in the  $p(\vec{e}, e'\vec{p})\pi^0$  reaction. These components exhibit strong sensitivities to the resonant Roper multipoles  $M_{1-}$  and  $S_{1-}$ . The measurements will offer a unique insight for extracting information on the  $N \rightarrow R$  transition through comparison with the state-of-the-art models, and will also provide severe constraints on these models in the second resonance region.

## 1 Introduction

The  $P_{11}(1440)$  (Roper) resonance [1] is the lowest positive-parity  $N^*$  state. It is visible in partial-wave decompositions of  $\pi N \rightarrow \pi N$  and  $\pi N \rightarrow \pi\pi N$  scattering [2,3] as a shoulder around 1440 MeV with a width of about 350 MeV [4]. Its large width causes it to merge with the adjacent  $D_{13}(1520)$  and  $S_{11}(1535)$  resonances, and therefore it can not be resolved from the  $W$ -dependence of the cross-section alone. A more selective and sensitive experiment has been designed in which the structure of the Roper will be probed by measuring the recoil proton polarization components  $P'_x$ ,  $P_y$ , and  $P'_z$  in the  $p(\vec{e}, e'\vec{p})\pi^0$  reaction at a specific value of  $Q^2$ ,  $W$  and centre-of-mass angle  $\theta$ . It is for the first time that the Roper resonance is being approached by means of the recoil-polarization technique, although this strategy benefits substantially from the experience gained in the well-studied  $N \rightarrow \Delta$  transition.

## 2 Relation to other experiments

The region of the Roper resonance has been explored to various extents in the past both at Jefferson Lab and MAMI. In most of the experiments, only cross-sections (angular distributions) were measured. Only a handful of single- and double-polarization measurements have been performed so far.

## 2.1 Jefferson Lab: Hall B (CLAS)

Kinematically most extensive data sets on single-pion electro-production in the nucleon resonance regions come from Hall B at JLab. Angular distributions and  $W$ -dependence of the electron beam asymmetry  $\sigma_{LT'}$  have been measured for both charged and neutral channels in the  $P_{33}(1232)$  region at  $Q^2 = 0.4$  and  $0.65$  (GeV/c)<sup>2</sup> [5,6]. Dispersion-relation (DR) techniques and unitary isobar models (UIM) have been applied to analyze the CLAS  $\sigma_{LT'}$  data in this range of  $Q^2$  and spanning also the second resonance region, in order to extract the contributions of the  $P_{33}(1232)$ ,  $P_{11}(1440)$ ,  $D_{13}(1520)$ , and  $S_{11}(1535)$  resonances to single-pion production [7].

A complete angular coverage was achieved, and several relevant amplitudes could be separated in a partial-wave analysis restricted to  $l \leq 2$ . The Legendre moments  $D_0$ ,  $D_1$ , and  $D_2$  of the expansions

$$\sigma_\alpha = D_0 + D_1 P_1(\cos \theta_\pi^*) + D_2 P_2(\cos \theta_\pi^*) + \dots$$

for different partial cross-sections  $\sigma_\alpha$  (or corresponding structure functions) were determined, e.g. for  $\sigma_\alpha \equiv \sigma_T + \varepsilon \sigma_L$ . To achieve a good fit of  $\theta_\pi^*$ - and  $W$ -dependence of  $\sigma_{LT'}$ , a simultaneous adjustment of the  $M_{1-}$  and  $S_{1-}$  amplitudes was needed. Since both the  $p\pi^0$  and the  $n\pi^+$  channel were measured, the transverse helicity amplitude  $A_{1-}^p \propto_p M_{1-}^{1/2}$  as well as the scalar  $S_{1-}^p \propto_p S_{1-}^{1/2}$  could be extracted. The results show a rapid fall-off of  $A_{1-}^p$  and indicate its zero-crossing at approximately  $Q^2 = 0.5$  (GeV/c)<sup>2</sup>.

In Hall B, there is also an approved experiment E03-105 [8] to measure single-pion photo-production in both  $p(\gamma, \pi^+)n$  and  $p(\gamma, p)\pi^0$  channels, with polarized beam and longitudinally and transversely polarized target using CLAS. It will measure two single- (T and P) and three double-polarization observables (G, F, and H); in addition, the experiment E01-104 will measure the double-polarization observable E. The measurements will span the range  $1300 \leq W \leq 2150$  MeV and achieve an angular coverage of  $-0.9 \leq \cos \theta^* \leq 0.9$ .

It is believed that this data will greatly constrain partial-wave analyses in photo-production and reduce model-dependent uncertainties in the extraction of nucleon resonance properties. A similar goal, but in electro-production, and utilizing the recoil-polarimetry technique, has been put forward by the Hall A Collaboration at JLab [9]. To some extent this experiment would be complementary to the effort with CLAS. However, due to Laboratory beam-time constraints, it has been deferred.

## 2.2 Jefferson Lab: Hall A

Polarized electron beam and recoil-polarimetry capability of Hall A also allow access to double-polarization observables in single-pion electro-production. Recoil-polarization observables are composed of different combinations of multipole amplitudes than observables accessible in the case of a polarized target.

The acceptance of CLAS is large enough to achieve a complete angular coverage of the outgoing hadrons. This is not possible in the case of relatively small

angular openings of the Hall A HRS spectrometers except at high  $Q^2$  where the Lorentz boost from the center-of-mass to lab frame focuses the reaction products into a cone narrow enough to provide a virtually complete out-of-plane acceptance. The E91-011 experiment in Hall A in the  $p(\vec{e}, e'\vec{p})\pi^0$  channel [10] was performed at sufficiently high  $Q^2 = (1.0 \pm 0.2) (\text{GeV}/c)^2$  and  $W = (1.23 \pm 0.02) \text{ GeV}$  to allow for a measurement of all accessible response functions, even those that vanish for coplanar kinematics. Two Rosenbluth combinations and 14 structure functions could be separated, allowing for a restricted partial-wave analysis giving access to all  $l \leq 1$  multipole amplitudes relevant to the  $N \rightarrow \Delta$  transition. Both multipoles indicate a rising trend approaching the  $W \sim 1440 \text{ MeV}$  region, again pointing towards the Roper.

Unfortunately, the cross-sections at  $W \sim 1440 \text{ MeV}$  (for any  $Q^2$ ) are about an order of magnitude smaller than in the  $\Delta$ -peak. For high  $Q^2 \sim 1 (\text{GeV}/c)^2$ , where a large out-of-plane coverage would allow for a decent partial-wave analysis in Hall A, the cross-sections are even smaller. Furthermore, due to the zero-crossing uncertainty of the  $M_{1-}$  multipole, it is not clear what value of  $Q^2$  to choose in order to have a prominent  $M1$  signal. Furthermore, models indicate that the crucial features of the Roper multipoles (or helicity amplitudes) are visible at relatively small  $Q^2$  of a few  $0.1 (\text{GeV}/c)^2$ , nullifying the boost-advantage of the HRS spectrometers.

We note in addition that higher partial waves ( $l \geq 2$ ) in all JLab partial-wave analyses so far needed to be constrained by models (just as in the CLAS experiments). Thus, even with (almost) complete angular coverages, existing data sets of finite statistical certainty do not allow for a “full” partial-wave analysis to sufficiently large  $l$ .

### 2.3 MAMI/A2

In photo-production, the double-polarization asymmetry  $G$  for linearly polarized photons ( $P_\gamma$ ) and target nucleons polarized longitudinally ( $P_z$ ) along the photon momentum, exhibits a very strong sensitivity to the Roper resonance. It is defined as

$$G = \frac{d\sigma(\Phi = 45^\circ, z) - d\sigma(\Phi = -45^\circ, z)}{d\sigma(\Phi = 45^\circ, z) + d\sigma(\Phi = -45^\circ, z)},$$

where  $\Phi$  is the angle between the photon polarization plane and the reaction plane. The cross-section has the form

$$d\sigma(\theta_\pi, \Phi) = d\sigma(\theta_\pi) \left( 1 - P_\gamma \Sigma(\theta_\pi) \cos 2\Phi + P_\gamma P_z G(\theta_\pi) \sin 2\Phi \right).$$

In the  $\vec{\gamma}p \rightarrow p\pi^0$  reaction,  $G$  depends on the interference of the much better-known  $M_{1+}$  multipole governed by the  $\Delta(1232)$ , and the  $M_{1-}$  driven by the Roper,

$$G(\theta_\pi) \simeq \sin^2 \theta_\pi \text{Im}M_{1+} \text{Re}M_{1-}.$$

The asymmetry  $G$  will be measured by virtue of its  $\sin 2\Phi$ -dependence at the A2 Collaboration at MAMI with the  $\Phi$ -symmetric detector DAPHNE. The expected sensitivity is shown in Fig. 1. In addition to the  $p\pi^0$ , the  $n\pi^+$  channel will be measured, allowing for the isospin decomposition of the partial waves.

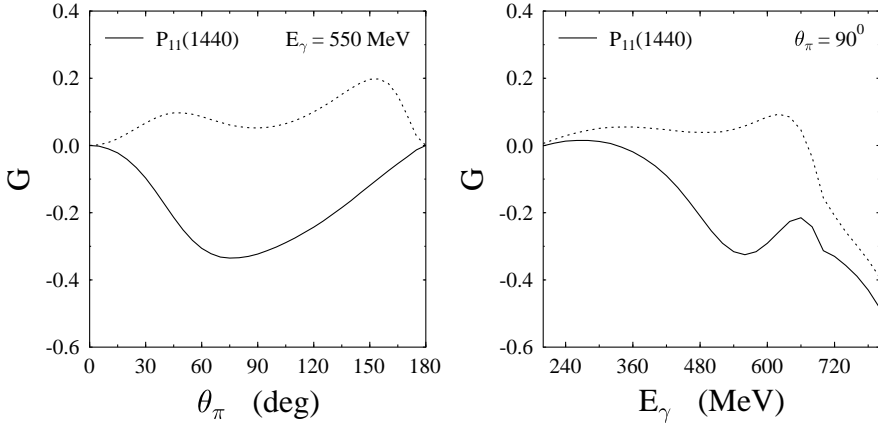


**Fig. 1.** MAID prediction for  $G$  in  $\bar{\gamma}p \rightarrow p\pi^0$ : angular distribution at  $W = 1440$  MeV and energy dependence at  $\theta_\pi = 90^\circ$ . The dotted curves correspond to the Roper switched off.

## 2.4 MAMI: A1

All three recoil polarization components ( $P'_x/P_e$ ,  $P_y$ , and  $P'_z/P_e$ ) in the  $p(\bar{e}, e'\bar{p})\pi^0$  reaction at the  $\Delta$  resonance, at  $Q^2 = 0.121$  (GeV/c) $^2$  have been measured by the A1 Collaboration at MAMI [11]. These components, in particular the  $P'_x$ , were shown to be highly sensitive to the Coulomb quadrupole to magnetic dipole ratio

$$\text{CMR} = \text{Im}S_{1+}^{(3/2)} / \text{Im}M_{1+}^{(3/2)}$$

in the  $N \rightarrow \Delta$  transition. (For the results of a similar, far more ambitious experiment at higher  $Q^2$  at JLab, see [12].)

## 3 Proposed measurement at MAMI/A1

A straight-forward extension of the  $N \rightarrow \Delta$  program in the  $\bar{p}\pi^0$  channel into the Roper region appears to be unfeasible at Mainz/A1 due to instrumental constraints. Wishing to cover a reasonably broad kinematic range in the Roper region, one typically encounters angular and momentum settings and focal-plane polarimetry conditions which are unfavourable for the A1 spectrometer setup (assuming the existence of a fully equipped and operational KAOS spectrometer).

However, a good compromise can be found by going to non-parallel (or non-anti-parallel) kinematics for the proton. By doing this, we sacrifice some of the high sensitivities to the inclusion/exclusion of the Roper seen in the predicted polarization components, but we tune the kinematics such that we balance well between the physics sensitivities and maintaining good figures-of-merit for the FPP, as well as satisfying all geometry and momentum requirements. We have proposed the following baseline kinematics:

$$E_e = 1500 \text{ MeV}, \quad Q^2 = 0.1 \text{ GeV}^2, \quad E'_e = 811 \text{ MeV}/c, \quad \theta_e = 16.5^\circ$$

for the electron (to be detected in Spectrometer B) and corresponding to an invariant mass of  $W = 1440 \text{ MeV}$ . The hadron kinematics was chosen to be at  $\theta_{\text{cms}} = 90^\circ$ , which translates into

$$p_p = 668 \text{ MeV}/c, \quad T_p = 214 \text{ MeV}, \quad \theta_p = 54.2^\circ$$

to be covered by Spectrometer A. The proton kinetic energy in the center of the carbon secondary scatterer in the FPP is then about  $T_{\text{cc}} \approx 200 \text{ MeV}$ , which translates into a favourable figure-of-merit (FOM) of about  $f_{\text{FPP}} \approx 0.006$ . The FOM drops to  $\approx 0.003$  for  $\theta \approx 75^\circ$ .

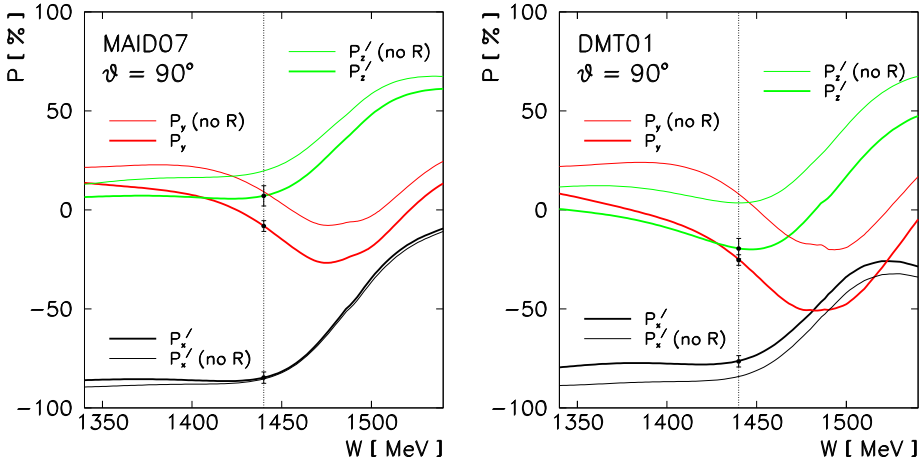


Fig. 2. Expected uncertainties on  $P'_x$ ,  $P_y$  and  $P'_z$  for 100 h beamtime;  $W$ -dependence.

The following estimates have been done with the dipole approximation for the precession matrix ( $\chi \approx 215^\circ$ ), assuming 100 h of  $10 \mu\text{A}$  beam with  $P_e = 75\%$  polarization on a  $5 \text{ cm}$   $\text{LH}_2$  target, and reasonably conservative cuts in the simulation. One obtains  $\approx 7000$  counts/hour (before the FPP cuts) and the error estimates (for  $\theta = 90^\circ$ )

$$\begin{aligned} \Delta P'_x &= \frac{1}{P_e} \sqrt{\frac{2}{N_0 f}} \approx 0.029 \\ \Delta P_y &= \frac{1}{\cos \chi} \sqrt{\frac{2}{N_0 f}} \approx 0.027 \\ \Delta P'_z &= \frac{1}{P_e} \frac{1}{\sin \chi} \sqrt{\frac{2}{N_0 f}} \approx 0.051 \end{aligned}$$

Figure 2 shows the level of accuracy that can be achieved under these assumptions for the polarization components  $P'_x$ ,  $P_y$  and  $P'_z$ , shown here as a function of  $W$ . One can see that we are sensitive mostly to transverse helicity amplitudes and that  $P'_x$  in some sense is useless except for calibration purposes.

### 3.1 Relation of polarization components to multipoles

The cross-section for the  $p(\vec{e}, e'\vec{p})\pi^0$ , allowing for both a polarized electron beam and detection of the recoil proton polarization, is given by

$$\frac{d\sigma}{dE'_e d\Omega_e d\Omega_p^*} = \frac{\sigma_0}{2} \left\{ 1 + \mathbf{P} \cdot \hat{\mathbf{s}}_r + h \left[ A_e + \mathbf{P}' \cdot \hat{\mathbf{s}}_r \right] \right\},$$

where  $\sigma_0 \equiv d\sigma(\hat{\mathbf{s}}_r) + d\sigma(-\hat{\mathbf{s}}_r)$  is the unpolarized cross-section,  $\hat{\mathbf{s}}_r$  is the proton spin vector in its rest frame,  $h$  is the helicity of the incident electrons,  $\mathbf{P}$  is the induced proton polarization,  $A_e$  is the beam analyzing power, and  $\mathbf{P}'$  is the vector of spin-transfer coefficients. The polarization of the recoiled proton consists of a helicity-independent (induced) and a helicity-dependent (transferred) part,  $\mathbf{\Pi} \equiv \mathbf{P} + h\mathbf{P}'$ . (Alternative notations for the polarization components is  $P'_x \leftrightarrow -P_t$ ,  $P_n \leftrightarrow P_y$ , and  $P'_z \leftrightarrow -P_l$ .)

The structure functions contain the following combinations of the multipoles relevant for the Roper (the corresponding polarization component is given in the bracket before the structure function):

$$(P_n)R_T^n = -\text{Im} E_{0+}^* (3E_{1+} + M_{1+} + 2M_{1-})$$

contains the leading  $M_{1-}$  amplitude in the imaginary part of the interference with the  $E_{0+}$  non-resonant amplitude; this is matched with the

$$(P_l)R_{TT}^l \propto \text{Re} E_{0+}^* (3E_{1+} + M_{1+} + 2M_{1-})$$

response which contains the real part of the same interference. The terms

$$(P_n)R_{TL}^n \text{ contains } \text{Im} L_{1-}^* M_{1-},$$

$$(P_l)R_{TL}^l \text{ contains } \text{Re} L_{1-}^* M_{1-}$$

contain (real and imaginary) interferences of both resonant multipoles but these probably have less relevance because both are very small. In addition, there are the

$$(P_n)R_L^n \propto -2 \text{Im} L_{0+}^* (2L_{1+} - L_{1-}),$$

$$(P_t)R_{TL}^t \propto \text{Re} \left\{ L_{0+}^* (2M_{1+} + M_{1-}) + (2L_{1+}^* - L_{1-}^*) E_{0+} + \dots \right\}$$

terms, as well as the  $(P_n)R_{TT}^n$  that contains  $\sin \theta \cos \theta M_{1+}^* M_{1-}$ . The latter term is not accessible at  $\theta = 90^\circ$ .

Even with only two angular points ( $\theta = 90^\circ$  and  $\theta = 75^\circ$ ), a strong physics case can be made. The experiment will possess enough power to distinguish between Roper on/off calculations in both MAID2007 and DMT2001 models at these kinematics. The differences in the models originate in different treatments of resonances in isobar models (like MAID) versus those of dynamical models (like DMT), that is, of having “dressed” vs. “bare” resonant vertices.

## References

1. L. D. Roper, Phys. Rev. Lett. **12** (1964) 340.
2. D. M. Manley, E. M. Saleski, Phys. Rev. D **45** (1992) 4002.
3. R. E. Cutkosky, C. P. Forsyth, R. E. Hendrick, R. L. Kelly, Phys. Rev. D **20** (1979) 2839.
4. S. Eidelman et al. (Particle Data Group), Phys. Lett. B **592** (2004) 1.
5. K. Joo et al. (CLAS Collaboration), Phys. Rev. C **68** (2003) 032201(R).
6. K. Joo et al. (CLAS Collaboration), Phys. Rev. C **70** (2004) 042201(R).
7. I. Aznauryan, V. D. Burkert, H. Egiyan, K. Joo, R. Minehart, L. C. Smith, Phys. Rev. C **71** (2005) 015201.
8. N. Benmouna, G. O'Rielly, I. Strakovski, S. Strauch, JLab Experiment E03-105.
9. O. Gayou, S. Gilad, S. Širca, A. Sarty (co-spokespersons), JLab Proposal PR05-010.
10. J. J. Kelly, A. Sarty, S. Frullani (co-spokespersons), JLab Experiment E91-011.
11. Th. Pospischil et al. (A1 Collaboration), Phys. Rev. Lett. **86** (2001) 2959.
12. J. J. Kelly et al. (Hall A Collaboration), Phys. Rev. Lett. **95** (2005) 102001; see also J. J. Kelly et al. (Hall A Collaboration), Phys. Rev. C **75** (2007) 025201.